

# Theoretical investigation on the structure and thermodynamic properties of the 2,4-dinitroimidazole complex with methanol

Shu-sen Zhao · Wen-jing Shi · Jian-long Wang

Received: 2 February 2012 / Accepted: 29 June 2012 / Published online: 29 July 2012  
© Springer-Verlag 2012

**Abstract** The structure and thermodynamic properties of the 2, 4-dinitroimidazole complex with methanol were investigated using the B3LYP and MP2(full) methods with the 6-31++G(2d,p) and 6-311++G(3df,2p) basis sets. Four types of hydrogen bonds [N–H···O, C–H···O, O–H···O (nitro oxygen) and O–H··· $\pi$ ] were found. The hydrogen-bonded complex having the highest binding energy had a N–H···O hydrogen bond. Analyses of natural bond orbital (NBO) and atoms-in-molecules (AIM) revealed the nature of the intermolecular hydrogen-binding interaction. The changes in thermodynamic properties from monomers to complexes with temperatures ranging from 200.0 to 800.0 K were investigated using the statistical thermodynamic method. Hydrogen-bonded complexes of 2,4-dinitroimidazole with methanol are fostered by low temperatures.

**Keywords** 2,4-Dinitroimidazole complex with methanol · Intermolecular hydrogen-binding interaction · Thermodynamic property · MP2(full)

**Electronic supplementary material** The online version of this article (doi:10.1007/s00894-012-1524-y) contains supplementary material, which is available to authorized users.

S.-s. Zhao  
Software School of North University of China,  
Taiyuan 030051, China

W.-j. Shi (✉)  
The Third Hospital of Shanxi Medical University,  
Taiyuan 030053, China  
e-mail: wenjingfd@126.com

J.-l. Wang  
College of Chemical Engineering and Environment,  
North University of China,  
Taiyuan 030051, China

## Introduction

Hydrogen bonds, which can be designated as D–H···A (D and A being donor and acceptor of proton, respectively), have received much attention recently as a result of their extremely important role in stabilizing crystal structures, in steering chemical and bio-chemical processes, and in influencing the movement and arrangement of molecules in gases, liquids and solids [1, 2]. For example, intermolecular hydrogen-bonding interactions between solute and solvent might play a role in the separation and purification of explosives [3–5]. It has been shown from many experimental and theoretical results that a favorable interaction between solute and solvent molecules is often associated with high yields and purity [4–10].

Nitroimidazole represents an important type of explosive. Nitroimidazoles have a heteroaromatic structure consisting of an imidazole-based nucleus with a nitro group and pyrrolic hydrogen that can participate in the formation of an intermolecular hydrogen-bonding interaction. As an energetic compound, most studies have focused mainly on the syntheses of novel nitroimidazole derivatives which have high energy while retaining low sensitivity [6, 9–12], and on theoretical investigations into structure, energy and stability [13–17]. Recently, many investigations into the solvent effects on the structures and activities of nitroimidazole compounds have also been carried out. Liu et al. [4] investigated the separation and purification processes of 2, 4-dinitroimidazole using methanol as a solvent. Ramalho et al. [15] calculated the electron affinity of nitroimidazole in water and carbon tetrachloride using Hartree–Fock (HF) and density functional theory (DFT) methods, and evaluated solvent effects on electron affinity. Cho et al. [16] used ab initio and DFT methods to study the stabilities and solvent

effects of nitroimidazole, and suggested that the solvent effect plays an important role in the relative stability of nitroimidazole in solutions.

It is well known that temperature is one of the key factors controlling the purity and yield of explosives during the separation and purification process. To obtain high yield and purity, it is necessary to study changes in stability thermodynamic properties with changes in temperature for the complex between the explosive and solvent molecules. However, to our knowledge, no theoretical investigation on changes in the thermodynamic properties of the complex between nitroimidazole and solvent molecules in response to changes in temperature has been presented.

2,4-Dinitroimidazole is a typical nitroimidazole compound consisting of N–H, C–H and two –NO<sub>2</sub> groups at different positions of an imidazole ring. Methanol is one of the simplest and most important polar organic solvents. The hydrogen bonds N–H···O, C–H···O, O–H···O and O–H···π (five-member π-ring) might form in the complex of 2,4-dinitroimidazole–methanol. Thus, the 2,4-dinitroimidazole complex with methanol can serve as a model system for a nitroimidazole–solvent interaction. In this paper, we examine the intermolecular hydrogen-bonding interaction of 2,4-dinitroimidazole with methanol, and investigate changes in the thermodynamic properties from the monomer to hydrogen-bonded complex in response to changes in temperature using statistical thermodynamic methods. These computations in vacuum will be very useful in gaining better insight into the solvation process and for further experimental study of the separation and purification of explosives.

### Computational details

As a cost-effective approach in most cases, geometry optimization by density functional theory (DFT) methodology is feasible and can be applied successfully to investigate the structure of complexes. However, to investigate complexation energy, the MP2(full) method is more reliable [18–21]. In addition, a high quality basis set is crucial for calculating the properties of the complex [22]. Here, we attempted to use the MP2(full)/aug-cc-pVTZ method to carry out geometrical optimization and evaluate the intermolecular interactions of 2,4-dinitroimidazole complexes; however, this proved too expensive. In fact, to investigate the energetic and thermodynamic properties of hydrogen-bonded complexes with methanol, the MP2(full)/6-311+G(3df,2p) method is now reliable enough [23–25]. Taking all the above factors into account, we decided to use the DFT-B3LYP and MP2(full) methods with the 6-311+G(2d,p) and 6-311+G(3df,2p) basis sets in this work.

All calculations were performed using Gaussian 03 programs [26]. Firstly, all possible orientations of methanol

towards 2,4-dinitroimidazole were fully optimized at the B3LYP/6-31++G(2d,p) level. The complexes obtained were then reoptimized, and the vibrational frequencies calculated at the MP2(full)/6-311++G(3df,2p) level. Complexes corresponding to the minimum energy points at the molecular energy hypersurface (NImag = 0) were obtained. Standard thermodynamic properties and changes in thermodynamic functions were predicted on the basis of vibrational analysis and statistical thermodynamics in order to investigate the thermodynamics of the binding process [27]. Since the calculated harmonic vibrational frequencies at the MP2(full)/6-311++G(3df,2p) level are usually larger than those observed experimentally, according to literature [28], a scaling factor of 0.9427 was used. Natural bond orbital (NBO) [29] analysis was carried out using the B3LYP/6-31++G(2d,p) method and the topological charge density was displayed by the AIM method [30] using the program [AIMPAC 31] at MP2(full)/6-311++G(3df,2p) level. Single energy calculations using B3LYP/6-31++G(2d,p), B3LYP/aug-cc-pVTZ, MP2(full)/6-31++G(2d,p) and MP2(full)/6-311++G(3df,2p) methods were carried out. Binding energy ( $D_e$ ) was expressed as follows:

$$D_e = E(\text{C}_3\text{H}_2\text{O}_4\text{N}_4 - \text{CH}_4\text{O}) - E(\text{C}_3\text{H}_2\text{O}_4\text{N}_4) - E(\text{CH}_4\text{O}) \quad (1)$$

$D_e$  corrected for basis set superposition error (BSSE) [32, 33] and zero-point energy correction (ZPEC) was evaluated.

### Results and discussion

In the conformational search, three kinds of conformations are taken into account. In the first, the O–H or C–H bond of methanol (donor of proton) points towards the oxygen or nitrogen atom of 2,4-dinitroimidazole. The second forms the T-shape, with the O–H or C–H bond of methanol (donor) lying perpendicular to the ring or C=C or C=N double bond of 2,4-dinitroimidazole and pointing toward to its midpoint. For the third type of conformation, the N–H or C–H bond of 2,4-dinitroimidazole (donor) points toward to the oxygen atom of methanol. At MP2(full)/6-311++G(3df,2p) level, only eight conformations are confirmed and will be described in some detail in the following section. For most of the predicted conformations, it is difficult to find local minima since the potential wells are flat.

The fully optimized structures and AIM results are shown in Fig. 1. The binding energies are listed in Table 1. Frequency shifts of the monomers in complexes and the results of the NBO analysis are given in Tables 2 and 3, respectively. The changes in thermodynamic properties are collected in Table 4.

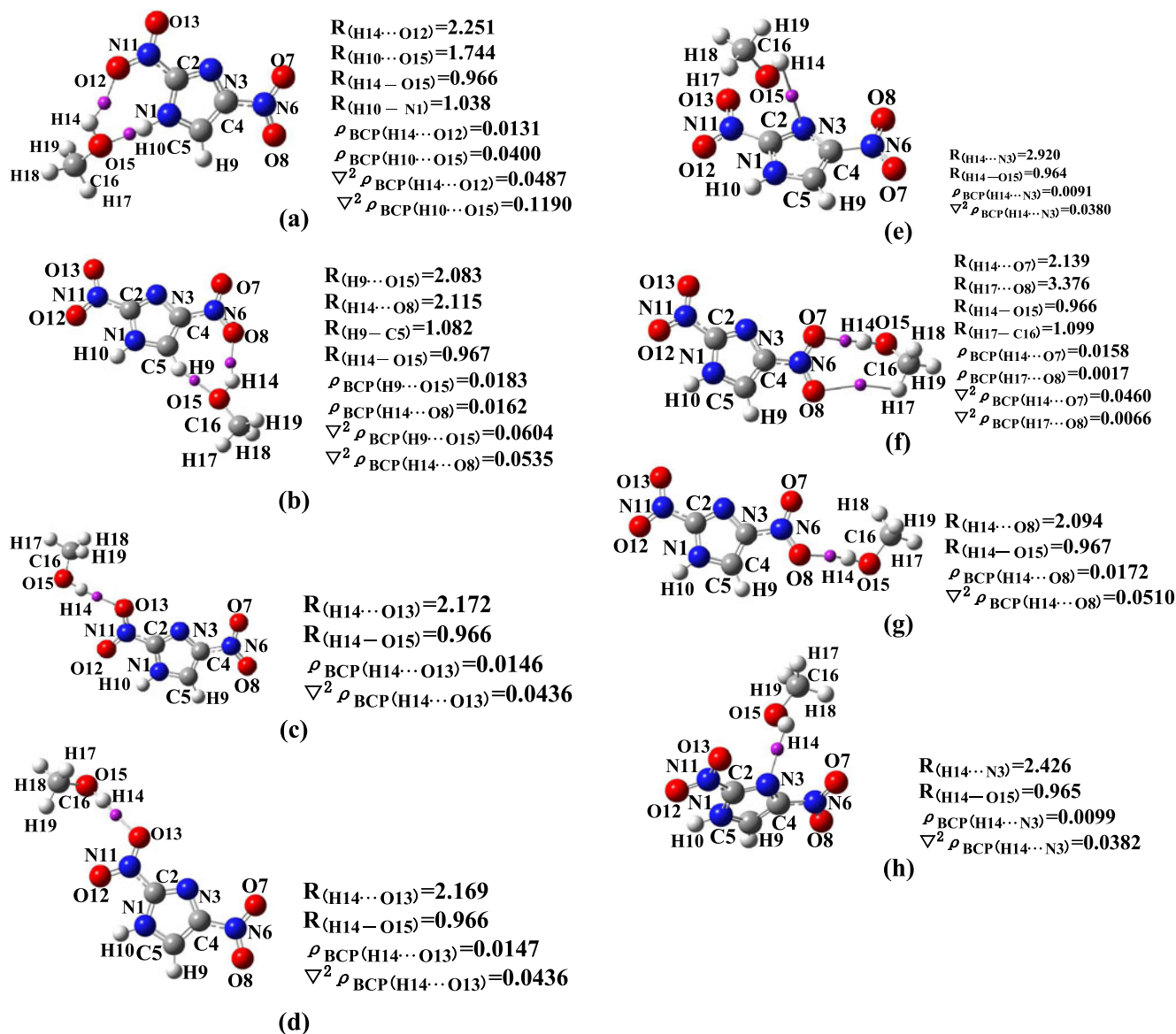


Fig. 1 a–h Molecular structures and bond critical points of the complexes at MP2(full)/6-311++G(3df,2p) level

**Table 1** Binding energies of complexes [ $-D_e$  (kJ mol<sup>-1</sup>)]. BSSE Basis set superposition error, ZPE zero-point energy

	B3LYP/6-31++G(2d,p)	B3LYP/aug-cc-pVTZ	MP2(full)/6-31++G(2d,p)	MP2(full)/6-311++G(3df,2p)
a <sup>a</sup>	44.70 (42.93) 37.87 <sup>b</sup>	43.43 (42.39) <sup>a</sup>	53.50 (45.14) <sup>a</sup>	56.38 (47.25) <sup>a</sup>
b	27.77 (26.80) 22.33	27.06 (26.27)	33.46 (27.10)	32.13 (28.16)
c	10.03 (9.80) 7.19	6.10 (5.56)	14.69 (11.21)	14.55 (12.34)
d	9.63 (9.07) 6.27	7.21 (6.62)	15.12 (11.20)	16.50 (11.47)
e	13.48 (12.18) 8.76	4.93 (4.14)	25.36 (18.94)	23.27 (19.10)
f	12.27 (11.68) 8.42	8.57 (7.94)	17.67 (13.59)	16.69 (13.22)
g	13.48 (12.94) 9.61	10.60 (10.03) <sup>a</sup>	18.36 (14.24)	18.37 (15.10)
h	14.98 (13.74) 10.65	9.28 (8.56)	28.37 (21.75)	27.22 (20.49)

<sup>a</sup>Values in parentheses are BSSE-corrected [ $-D_e(\text{BSSE})$ ]

<sup>b</sup>Binding energy is  $\Delta E$  with ZPE and BSSE ( $-D_e(\text{BSSE}, \text{ZPE})$ ) correction

<sup>a</sup>Complexes a–h as in Fig. 1

**Table 2** Selected frequency shifts of monomers in complexes **a–h** at MP2(full)/6-311++G(3df,2p) level <sup>a</sup>

	<b>a</b>	<b>b</b>	<b>c</b>	<b>d</b>	<b>e</b>	<b>f</b>	<b>g</b>	<b>h</b>
$\nu_1$	−47 (0.08)	−62 (0.26)	−30 (0.78)	−41 (1.74)	−48 (0.28)	−59 (0.33)	−61 (0.27)	−32 (0.19)
$\nu_2$	0 (0.87)	6 (0.13)	10 (0.42)	11 (0.59)	11 (0.22)	10 (0.64)	9 (0.47)	7 (0.19)
$\nu_3$	−2 (0.15)	7 (0.88)	5 (0.29)	9 (0.28)	5 (0.65)	11 (0.57)	10 (0.19)	1 (0.30)
$\nu_4$	−316 (0.00)	4 (0.22)	−1 (0.35)	−1 (0.39)	2 (0.65)	−1 (0.98)	−1 (0.29)	2 (0.63)
$\nu_5$	−176 (1.09)	−77 (0.20)	−1 (0.06)	−1 (0.09)	−1 (0.01)	−1 (0.08)	−1 (0.08)	1 (0.09)
$\nu_7$	−2 (0.39)	−7 (0.28)	−6 (0.35)	−8 (0.29)	−6 (0.55)	−8 (0.68)	−2 (0.26)	−2 (0.54)
$\nu_8$	13 (0.88)	−10 (0.11)	20 (0.43)	19 (0.09)	13 (0.26)	4 (0.55)	23 (0.54)	2 (0.39)

<sup>a</sup> All frequency shifts ( $\nu$ ) are in  $\text{cm}^{-1}$ ; values in parentheses are relative intensity of IR

### Structure of the complex

From Fig. 1, for complex (**a**), the O12 $\cdots$ O15 and O15 $\cdots$ N1 distances are 2.936 and 2.777 Å at the MP2(full)/6-311++G(3df,2p) level, respectively, i.e., shorter than the sum of the related van der Waals radii [34]. The corresponding bond angles ( $\angle\text{OHO}$  and  $\angle\text{OHN}$ ) are larger than  $90^\circ$  ( $127.0^\circ$  and  $172.7^\circ$ ). Therefore, the intermolecular hydrogen bonds O12 $\cdots$ H14–O15 and O15 $\cdots$ H10–N1 are suggested [34, 35]. As a result, the bond lengths of N1–H10, N11–O12, O15–H14 and C16–O15 are lengthened. The length of the N1–H10 bond is changed greatly, while that of O15–H14 bond is changed only slightly, showing that the N–H $\cdots$ O hydrogen bonding interaction might be dominant. The distances of the O $\cdots$ H hydrogen-bonds in O12 $\cdots$ H14–O15 and O15 $\cdots$ H10–N1 are 2.251 and 1.744 Å, respectively, at MP2(full)/6-311++G(3df,2p) level. We also obtained the O12 $\cdots$ H14 and O15 $\cdots$ H10 distances (2.242 and 1.728 Å) at B3LYP/6-31++G\*\* level. Fang et al. [5] calculated the complex of 3-nitro-1,2,4-triazol-5-one (NTO) with  $\text{NH}_3$  and  $\text{H}_2\text{O}$  at B3LYP/6-311++G\*\* level. They found that the O $\cdots$ H distances in O–H $\cdots$ O and N–H $\cdots$ O hydrogen bonds were 2.369 and 1.795 Å, respectively, which is close to our results, showing that the calculated structure of complex (**a**) in this paper is reliable.

In complex (**b**), the C–H $\cdots$ O hydrogen bond is found, as can also be confirmed by the O15 $\cdots$ C5 distance (3.085 Å) and corresponding bond angle ( $\angle\text{OHC}=152.8^\circ$ ). The C5–H9 bond is lengthened from 1.079 to 1.082 Å. The O–H $\cdots$ O (nitro oxygen) hydrogen bond is also observed in this complex, and the bond lengths of O15–H14 and N6–O8 are lengthened from 0.965 and 1.231 Å to 0.967 and 1.236 Å, respectively. The length of the C5–H9 bond is changed more than that of O15–H14, showing that, in (**b**), C–H $\cdots$ O hydrogen-bonding interactions might be dominant.

In complexes (**c**)–(**g**), O–H $\cdots$ O (nitro oxygen) hydrogen bonds are found. For complexes (**c**) and (**d**), intermolecular hydrogen-bonding interactions are both observed between O13 and H14. The hydrogen bond distance and structure of the two monomers in (**c**) and (**d**) are very close, with only

the methyl group attached to atom O15 in complex (**d**) moving to the opposite direction in complex (**c**). The O $\cdots$ H bond distances of are 2.172 and 2.169 Å in (**c**) and (**d**), respectively. In complex (**e**), a hydrogen-bonding interaction is found between N3 and H14. The whole methyl group and atom O15 lie over the 2,4-dinitroimidazole plane. The N $\cdots$ H distance is 2.920 Å. In complex (**f**), a hydrogen-bonding interaction is found between O7 and H14. In complex (**g**), the O–H $\cdots$ O hydrogen bond is also observed. The N6–O8 bond is lengthened from 1.231 to 1.235 Å.

In complex (**h**), the O–H $\cdots$  $\pi$  hydrogen bond is formed through the  $\pi$  electrons coming from the conjugation ring. The O15–H14 bond lies over the 2,4-dinitroimidazole and the distance of atom H14 to the closest atom N3 or C4 is 2.426 or 2.947 Å. The H14 atom almost points toward to the midpoint of the N3–C4 bond, similar to the X–H $\cdots$  $\pi$  (X=F; Cl; C) hydrogen bond in pyrrole–HCl (HF,  $\text{CHCl}_3$ ) and benzene–HF complexes [36–38].

The bonds involved in the formation of these hydrogen bonds change while the others are almost consistent with those in monomers, suggesting that the hydrogen-bonding interaction might be dominant in the title complexes. The N–H bond length in complex (**a**) is changed greatly while those of the O–H and N–O bonds in all complexes are changed only slightly, showing that the hydrogen-bonding interaction of N–H $\cdots$ O in complex (**a**) might be strongest.

### Energies and stabilities

Table 1 gives both uncorrected and corrected binding energies after correction of ZPE and BSSE by means of the counterpoise method. For (**a**), the interaction energy after the correction of the BSSE amounts to 42.93  $\text{kJ mol}^{-1}$  with B3LYP/6-31++G(2d,p) method and 47.25  $\text{kJ mol}^{-1}$  at MP2(full)/6-311++G(3df,2p) level, respectively. There is no direct measure of the interaction energy for the system, but values of 38.53 and 37.45  $\text{kJ mol}^{-1}$  are reported in the literature, using the B3LYP/6-311++G\*\* method for NTO dimers in which the same hydrogen bonds as the complex of 2,4-dinitroimidazole with methanol are formed [39].

**Table 3** Calculated parameters of complex at their equilibrium geometries: NBO occupation numbers for the oxygen or nitrogen n(p) lone pairs and n(s,p) and the (X–H)\* (X = N; C; O) antibonds, their respective orbital energies  $\epsilon$ , the second-order perturbation energies  $E^{(2)}$  and NBO charges of CH<sub>4</sub>O in its complexes (Q) at B3LYP/6-31++G(2d,p) level

	a	b	c	d	e	f	g	h
Occ.n(p) <sup>a</sup>	1.9050 sp <sup>99,99</sup>	1.9037 sp <sup>99,99</sup>	1.8858 sp <sup>99,99</sup>	1.8850 sp <sup>99,99</sup>	1.8937 sp <sup>99,99</sup>	1.8907 sp <sup>99,99</sup>	1.8998 sp <sup>99,99</sup>	
$\epsilon$ {n(p)} <sup>b</sup>	-0.3417	-0.3339	-0.3489	-0.3487	-0.3276	-0.3357	-0.3388	
Occ.n(s,p) <sup>a</sup>	1.9320 sp <sup>3,75</sup>	1.9726 sp <sup>1,09</sup>						1.9033 <sup>d</sup> sp <sup>1,97</sup>
$\epsilon$ {n(s,p)} <sup>b</sup>	-0.4911	-0.6227						-0.4372 <sup>d</sup>
Occ.(C/N–H) <sup>*a</sup>	0.0612	0.0212						
$\epsilon$ {(C/N–H)*} <sup>b</sup>	0.3607	0.3960						
Occ.(O–H) <sup>*a</sup>	0.0087	0.0121	0.0139	0.0138	0.0114	0.0152	0.0162	0.0085
$\epsilon$ {(O–H)*} <sup>b</sup>	0.3877	0.4245	0.4595	0.4575	0.4482	0.4653	0.4644	0.4370
$E^{(2)}$ <sub>n(p)→(O–H)*<sup>c</sup></sub>	2.56	6.61	9.74	9.07	3.55	11.12	11.92	
$E^{(2)}$ <sub>n(s,p)→(C/N–H)*<sup>c</sup></sub>	85.94	20.32						1.55
Q(CH <sub>4</sub> O) <sup>e</sup>	45.2	7.8	-8.8	-8.8	-3.5	-11.2	-11.5	-0.7

<sup>a</sup> Occ.: occupation number

<sup>b</sup> In a.u.

<sup>c</sup> In kJ mol<sup>-1</sup>

<sup>d</sup> For the atom N3

<sup>e</sup> In me

**Table 4** Thermodynamic properties of 2, 4-dinitroimidazole (2,4-DNI), CH<sub>3</sub>OH and 2,4-DNI/CH<sub>3</sub>OH at different temperatures at MP2(full)/6-311++G(3df,2p) level <sup>a</sup>

Structure	Temperature/(K)	$C_{p,m}^{\theta}/(\text{J mol}^{-1} \text{K}^{-1})$	$S_m^{\theta}/(\text{J mol}^{-1} \text{K}^{-1})$	$H_m^{\theta}/(\text{kJ mol}^{-1})$	$\Delta S_T/(\text{J mol}^{-1} \text{K}^{-1})$	$\Delta H_T/(\text{kJ mol}^{-1})$	$\Delta G_T/(\text{kJ mol}^{-1})$
2,4-DNI (1)	200.0	102.04	346.01	13.51			
	298.15	134.15	391.15	24.97			
	400.0	168.09	437.54	40.94			
	600.0	213.39	515.16	79.75			
	800.0	240.22	580.83	127.31			
CH <sub>3</sub> OH (2)	200.0	39.93	221.35	7.32			
	298.15	45.17	237.26	11.66			
	400.0	54.12	252.63	16.72			
	600.0	70.03	277.81	29.65			
	800.0	82.65	299.54	45.26			
<b>a</b>	200.0	151.01	439.20	22.53	-128.16	-37.83	-12.20
	268.0	181.98	489.52	34.92	-123.52	-37.22	-4.12
	298.15	192.45	506.93	40.21	-121.48	-36.71	-0.49
	323.0	205.86	553.21	46.63	-119.25	-36.42	2.08
	400.0	236.97	572.18	65.27	-117.99	-35.53	11.67
<b>b</b>	600.0	299.98	681.27	124.46	-111.70	-32.86	34.16
	800.0	342.54	775.18	194.28	-105.19	-30.23	53.92
	200.0	154.82	451.20	23.09	-116.16	-20.91	2.32
	298.15	194.50	518.92	42.12	-109.49	-19.63	13.01
	400.0	238.62	585.36	66.71	-104.81	-18.12	23.80
<b>c</b>	600.0	301.71	695.28	125.82	-97.69	-15.68	42.93
	800.0	342.89	788.31	197.18	-92.06	-13.10	60.55
	200.0	155.96	486.19	24.12	-81.17	-5.65	10.58
	298.15	196.02	555.60	43.27	-72.81	-4.23	17.48
	400.0	239.82	623.65	67.60	-66.52	-3.01	23.60
<b>d</b>	600.0	302.13	733.21	127.15	-59.76	-0.13	35.73
	800.0	343.45	826.19	198.71	-54.18	3.29	46.63
	200.0	155.87	485.22	24.55	-82.14	-5.42	11.01
	298.15	195.66	552.69	43.72	-75.72	-4.09	18.49
	400.0	239.79	620.35	67.63	-69.82	-2.73	25.20
<b>e</b>	600.0	302.05	731.58	127.59	-61.39	0.12	36.95
	800.0	343.41	824.77	198.95	-55.60	3.53	48.01
	200.0	155.83	464.79	23.65	-102.57	-8.62	11.89
	298.15	195.59	532.37	42.58	-96.04	-7.36	21.27
	400.0	239.72	600.12	67.08	-90.05	-6.03	29.99
<b>f</b>	600.0	301.96	710.28	126.51	-82.69	-3.25	46.36
	800.0	343.38	804.57	198.06	-75.80	-0.32	60.32
	200.0	155.26	472.61	23.83	-94.75	-7.26	11.69
	298.15	195.47	540.11	42.72	-88.30	-6.10	20.23
	400.0	239.65	608.02	67.31	-82.15	-4.72	28.14
<b>g</b>	600.0	301.93	718.53	126.68	-74.44	-1.96	42.70
	800.0	343.29	812.28	198.17	-68.09	1.16	55.63
	200.0	154.82	479.26	23.77	-88.10	-8.62	9.00
	298.15	194.95	546.39	42.76	-82.02	-7.30	17.15
	400.0	239.05	614.55	67.55	-75.62	-6.61	23.64
<b>h</b>	600.0	301.59	725.01	126.67	-67.96	-3.38	37.40
	800.0	343.18	818.62	198.18	-61.75	-0.47	48.93
	200.0	155.98	450.29	23.84	-117.07	-10.22	13.19



**Table 4** (continued)

Structure	Temperature/(K)	$C_{p,m}^\theta$ /(Jmol <sup>-1</sup> K <sup>-1</sup> )	$S_m^\theta$ /(Jmol <sup>-1</sup> K <sup>-1</sup> )	$H_m^\theta$ /(kJmol <sup>-1</sup> )	$\Delta S_T$ /(Jmol <sup>-1</sup> K <sup>-1</sup> )	$\Delta H_T$ /(kJmol <sup>-1</sup> )	$\Delta G_T$ /(kJmol <sup>-1</sup> )
	298.15	195.86	538.37	42.85	-90.04	-8.75	18.10
	400.0	239.73	606.58	67.52	-83.59	-7.29	26.15
	600.0	302.86	716.52	126.98	-76.45	-4.53	41.34
	800.0	343.55	810.37	198.29	-70.00	-1.56	54.44

$${}^a \Delta S_T = (S_T^\theta)_k - (S_T^\theta)_1 - (S_T^\theta)_2, \Delta H_T = (H_m^\theta + E(\text{MP2}(\text{full})) + \text{ZPE})_k - (H_m^\theta + E(\text{MP2}(\text{full})) + \text{ZPE})_1 - (H_m^\theta + E(\text{MP2}(\text{full})) + \text{ZPE})_2$$

(k = (a)–(h))

Compared to the results mentioned above, the values calculated for complex **(a)** in this paper are reliable. For **(b)**, the interaction energy is 28.16 kJ mol<sup>-1</sup> at the MP2(full)/6-311++G(3df,2p) level, which is weaker than that of the complex **(a)**. For the remaining complexes, the intermolecular hydrogen-bonding interactions are no more than 21.00 kJ mol<sup>-1</sup> after the correction of BSSE at MP2(full)/6-311++G(3df,2p) level. These results show that the hydrogen-bonding interactions that the nitro oxygen participates in are weak. This result is consistent with the study on intermolecular interactions of NTO dimers [39].

As can be seen from Table 1, all the binding energies obtained at all four levels are almost in the same order: **(a)** > **(b)** > **(h)** > **(f)** > **(d)** ≈ **(c)** < **(g)** using the B3LYP method, while **(e)** > **(g)** employing the MP2(full) method. At MP2(full)/6-311++G(3df,2p) level, the order is **(a)** > **(b)** > **(h)** > **(e)** > **(g)** > **(f)** > **(d)** > **(c)**.

The proportion of correlated interaction energies for the complex to their total binding energies, defined as  $[(-D_e) - (-D_{e(\text{BSSE/ZPE})})]/(-D_e)$ , are up to 9.6 %, 16.0 %, 25.9 % and 30.5 % at the B3LYP/6-31++G(2d,p), B3LYP/aug-cc-pVTZ, MP2(full)/6-31++G(2d,p) and MP2(full)/6-311++G(3df,2p) levels for BSSE corrections, respectively. This indicates the necessity of checking the BSSE corrections for the MP2(full) method. In fact, the BSSE corrections for intermolecular interaction energies are not negligible. There is a standard computational protocol that requires BSSE corrections for intermolecular interaction energies: only in the case of the complete basis set, is the correction for BSSE not needed. On the other hand, ZPE corrections for the binding energies, which are up to 30.9 %, are larger than those of BSSE, suggesting that ZPE correction is also necessary for B3LYP/6-31++G(2d,p) methods.

#### Vibration frequencies

The larger the frequency shifts, the more stable the complex, so in this paper we have shown some important frequency shifts in order to investigate the relative stabilities of the complexes. The most important three vibrational frequencies of methanol,  $\nu_1$ ,  $\nu_2$  and  $\nu_3$ , can be described

approximately as the stretching of O–H, in-plane wagging vibration of O–H and stretching mode of C–O bond, respectively. From Table 2,  $\nu_1$  decreased (red shifts) while  $\nu_2$  and  $\nu_3$  increased (blue shifts) in the complexes **(b)**–**(h)**, indicating the formation of hydrogen bonds. For  $\nu_1$ , the frequency shifts in complexes **(c)** and **(d)** are the least except for **(h)**, suggesting that **(c)** and **(d)** are unstable, which is in agreement with analysis of the binding energy.

The selected vibrational frequency shifts of 2,4-dinitroimidazole are also shown in Table 2.  $\nu_4$  and  $\nu_5$  can be described approximately as the stretching frequencies of N1–H10 and C5–H9, respectively.  $\nu_6$  and  $\nu_7$  can be described approximately as the anti-symmetric and symmetric stretching vibration of two NO<sub>2</sub> groups. From Table 2, the  $\nu_4$  and  $\nu_5$  in complexes **(c)**–**(h)** are hardly changed; however, they decrease greatly in **(a)**, as does  $\nu_5$  in **b**, showing that the N–H⋯O [in **(a)**] and C–H⋯O [in **(b)**] hydrogen bonds are strong. This result is consistent with the analyses of geometries and binding energies. The  $\nu_6$  and  $\nu_7$  of 2,4-dinitroimidazole in **(c)**–**(h)** are changed slightly, showing that the O–H⋯π and O–H⋯O (nitro oxygen) hydrogen bonds that nitro oxygen participates in are weak, which is also in accordance with the geometries and binding energies analyses.

#### NBO analysis

According to the NBO analysis, all the complexes have two units, which is in agreement with the character of most intermolecular interactions. Delocalization effects between these two units can be identified from the presence of off-diagonal elements of the Fock matrix in the NBO basis, and the strengths of these delocalization interactions,  $E^{(2)}$  [29], can be estimated by second-order perturbation theory.

From Table 3, the results of  $E^{(2)}$  indicate that in complex **(a)**, the major interaction is that O15 (hydroxyl group) offers its lone pairs to the contacting  $\sigma(\text{N–H})^*$  antibond; this interaction stabilizes the system by 85.94 kJ mol<sup>-1</sup>. In **(b)**, the major intermolecular interaction is that the O15 offers its lone pairs to the  $\sigma(\text{C–H})^*$  antibond and this stabilizes the system by 20.32 kJ mol<sup>-1</sup>. In complex **(c)**–**(g)**, the major interactions are that the nitro oxygen atoms offer their p

electrons to the  $\sigma(\text{O-H})^*$  of methanol, and these stabilize the system by 9.74, 9.07, 3.55, 11.12 and 11.92 kJ mol<sup>-1</sup>, respectively. For complex **(h)**, the major interaction is that the  $\pi$  electrons coming from five-member  $\pi$ -ring transfers to the  $\sigma(\text{O-H})^*$  of methanol. As a result, the electrons in systems **(a)** and **(b)** transfer from methanol to 2,4-dinitroimidazole, while in complexes **(c)**–**(h)**, electrons transfer from 2,4-dinitroimidazole to methanol. The  $E^{(2)}$  values from the  $n(s,p) \rightarrow (N/C-H)^*$  interactions in **(a)** and **(b)** are higher than those of  $n(p) \rightarrow (\text{O-H})^*$  in **(c)**–**(g)**, which is in accordance with analyses of binding energies and geometries.

### AIM analysis

It is well known that electronic characteristics are essential to revealing the nature of intermolecular hydrogen-bonded interactions. As an advanced method that can offer a simple, rigorous and elegant way of partitioning any system into its atomic fragments, considering the gradient vector field of its electron density, Bader's atoms in molecules (AIM) theory has been applied widely to study intermolecular interactions [30].

According to AIM analysis at MP2(full)/6-311++G(3df,2p) level, there is a bond path linking the H9, H10 or H14 atom with the oxygen atom of the hydroxyl or nitro group accompanied by a BCP (see Fig. 1). Also, the values of the electron densities  $\rho_{\text{BCP}}$  obtained are within the range of 0.0091–0.0400 a.u., which just falls into the common accepted values for H-bonds (0.002–0.04 a.u.) [30]. Furthermore, the values of their Laplacians  $\nabla^2\rho_{\text{BCP}}$  are all positive. These results indicate the typical closed-shell kinds of interactions in these complexes. In other words, the small  $\rho_{\text{BCP}}$  and positive  $\nabla^2\rho_{\text{BCP}}$  values are basically similar to the topological properties of normal hydrogen bonds. Thus, the hydrogen bonds N–H $\cdots$ O, C–H $\cdots$ O and O–H $\cdots$ O (nitro oxygen) are confirmed. The largest  $\rho_{\text{BCP}}$  value was found to be 0.0400 a.u. in complex **(a)**, indicating that the interaction in **(a)** is the strongest, which is in accordance with the analyses of the structure, energy, frequency and NBO.

### Thermodynamic properties

The standard thermodynamic properties, such as heat capacities ( $C_{p,m}^\theta$ ), entropies ( $S_m^\theta$ ) and enthalpies ( $H_m^\theta$ ), are listed in Table 4. From Table 4, the calculated and experimental data are basically consistent. Taking methanol as an example, the calculated heat capacity is 45.17 J mol<sup>-1</sup> K<sup>-1</sup> at 298.15 K, which is close to the experimental value of 44.09 J mol<sup>-1</sup> K<sup>-1</sup> at the same temperature [40], indicating that theoretical computations using the MP2(full)/6-311++G(3df,2p) method are reliable. In order to evaluate the influence of temperature on the thermodynamic properties, the changes in the enthalpies ( $\Delta H_T$ ) and Gibbs free energies ( $\Delta G_T$ ) for the process from monomers to hydrogen-bonded complexes were calculated at different temperatures.

These calculated thermodynamic properties will be helpful for further studies on the physical and chemical properties, and separation and purification, of explosive molecules.

As can be seen from Table 4, the standard thermodynamic properties ( $C_{p,m}^\theta, S_m^\theta, H_m^\theta$ ) for monomers and complexes all increase clearly as the temperature increases. However, on going from monomers to supermolecules, the changes in entropy and enthalpy favor negative at any temperature from 200.0 to 600.0 K. The intermolecular interaction is therefore an exothermic process accompanied by a decrease in systematic entropy, and the negative enthalpy changes suggest that all the binding processes of intermolecular hydrogen-bond formations are enthalpically favorable in nature.

Since the value of  $\Delta H_T$  is insensitive to temperature, according to the equation  $\Delta G_T = \Delta H_T - T\Delta S_T$  by the ideal-gas model, the effect of temperature upon  $\Delta G_T$  is derived mainly from the contributions of the  $T\Delta S_T$  term, so the  $\Delta G_T$  value decreases when the temperature falls. Thus, the intermolecular interaction becomes stronger as the temperature decreases. For example, when the temperature is 400.0 K, the  $\Delta G_T$  of the formation process for **(a)** is 11.67 kJ mol<sup>-1</sup>, while the temperature decreases to 298.15 K, the  $\Delta G_T$  reduces to -0.49 kJ mol<sup>-1</sup>. It is clear that, when the temperature decreases from 400.0 K to room temperature, the intermolecular interaction between 2,4-dinitroimidazole and methanol becomes strong enough to form supermolecules via a spontaneous process, which is in accordance with the literature [4]. Furthermore, a negative value of  $\Delta G_T$  is observed at room temperature only for complex **(a)**, showing that only **(a)** can be produced spontaneously at room temperature. It was noted that, for the hydrogen-bonded complexes, there is no significant correlation between the experimental gas phase entropies and calculated entropies in vacuum when the vibrational frequencies are calculated in the harmonic approximation. Harmonic approximation is inadequate for the low-frequency vibrations that contribute significantly to vibration entropy. Therefore,  $\Delta S$  is usually too negative and therefore  $\Delta G$  too positive. In solution, the situation is more complex since solvation of the solutes by the solvent significantly restricts their mobility and freedom of rotation, so that the translation and rotation entropy calculated in the gas phase should be of low significance in solution. Therefore, the calculated  $\Delta G_T$  is more qualitative than quantitative and the calculated range of temperature where  $\Delta G_T < 0$  is inaccurate.

The equilibrium constant ( $K_T$ ) for the process from the monomer to complex **(a)** is predicted to be 6.354 and 1.219 with MP2(full)/6-311++G(3df,2p) method at 1 atm at temperatures of 268.0 and 298.15 K, respectively. However, when the temperature rises to 323.0 K, the Gibbs free energy tends towards positive, with the equilibrium constant 0.461 and complex **(a)** will decompose spontaneously. Over quite a short range of temperature, the equilibrium constant changes so much that, at 268.0 K, it is approximately 14



times greater than that at 323.0 K. Here, it should also be noted that, as mentioned above, there is no significant correlation between experimental and calculated complex entropies when vibrational frequencies are calculated in the harmonic approximation. Thus, the calculated  $K_T$  is also more qualitative than quantitative.

In addition, it is worth mentioning that, at the same temperature, the magnitude of the  $\Delta H_T$  or  $\Delta G_T$  is in the same following order: **(a)** < **(b)** < **(g)** < **(h)** < **(c)**  $\approx$  **(d)** < **(e)**, which is almost in agreement with the order of binding energies at the B3LYP/aug-cc-pVTZ level. This result indicates that intermolecular hydrogen bonding has a great influence on thermodynamic properties.

## Conclusions

B3LYP and MP2(full) calculations on the intermolecular hydrogen-bonding system of 2,4-dinitroimidazole with methanol were carried out. Four types of hydrogen bonds (N–H $\cdots$ O, C–H $\cdots$ O, O–H $\cdots$ O and O–H $\cdots$  $\pi$ ) were found. For the hydrogen-bonded complex with the highest binding energy, there is a N–H $\cdots$ O hydrogen bond. In complexes **(a)** and **(b)**, the hydroxyl oxygen offers lone pairs to the contacting  $\sigma(\text{N–H})^*$  or  $\sigma(\text{C–H})^*$  antibond orbital of the 2,4-dinitroimidazole. In complexes **(c)**–**(g)**, the nitro oxygen offers p electrons to the contacting  $\sigma(\text{O–H})^*$  antibond orbital of hydroxyl group, and five-member  $\pi$ -ring offers part of the  $\pi$  electrons to the  $\sigma(\text{O–H})^*$  antibond orbital of hydroxyl group in complex **(h)**. The hydrogen-bonded complexes of 2,4-dinitroimidazole with methanol are fostered by low temperatures.

## References

- Desiraju GR, Steiner T (1999) The weak hydrogen bond in structural chemistry and biology. Oxford University Press, New York
- Cao D, Ren F, Feng X, Wang J, Li Y, Hu Z, Chen S (2008) J Mol Struct THEOCHEM 849:76–83
- Bulusu S, Damavarapu R, Autera JR, Behrens R Jr, Minier LM, Villanueva J, Jayasuriya K, Axenrod T (1995) J Phys Chem 99:5009–5015
- Liu HJ, Yang L, Cao DL (2005) J Energetic Mat 13:141–143
- Fang GY, Xu LN, Xiao HM, Ju XH (2005) Acta Chim Sinica 63:1055–1061
- Hrelia P, Fimognary C, Maffei F, Brighenti B, Garuti L, Bumelli S, Cantelli-Forti G (1998) Mutat Res 397:293–301
- Suwinski J, Salwinska E (1987) Pol J Chem 61:613–920
- Grimmett MR, Hua ST, Chang KC, Foley SA, Simpson J (1989) Aust J Chem 42:1281–1289
- Li ZJ, Chu TW, Liu XQ, Wang XY (2005) Nucl Med Biol 32:225–231
- Anderson C, Beauchamp A (1995) Inorg Chim Acta 233:33–41
- Cho SG, Cheun YG, Park BS (1998) J Mol Struct THEOCHEM 432:41–53
- Cho SG, Park BS (1999) Int J Quantum Chem 72:145–154
- Gamézo VN, Odier S, Blain M, Fliszár S, Delpuech A (1995) J Mol Struct THEOCHEM 337:189–197
- Flammang R, Elguero J, Le HT, Gerbaux P, Nguyen MT (2002) Chem Phys Lett 356:259–266
- Ramalho TC, de Alencastro RB, La-Scalea MA, Figueroa-Villar JD (2004) Biophys Chem 110:267–279
- Cho SG, Cho JR, Park BS, Park GJ (2000) Mol Struct THEOCHEM 532:279–286
- Breccia A, Cavalleri B, Adams GE (eds) (1982) Nitroimidazoles. Chemistry, pharmacology, and clinical application. Plenum, New York
- Richard RM, Ball DW (2007) J Mol Struct THEOCHEM 806:113–120
- Macias AT, Norton JE, Evanseck JD (2003) J Am Chem Soc 125:2351–2360
- Suwattanamala A, Magalhaes AL, Gomes JANF (2005) Chem Phys 310:109–122
- Ruan C, Yang Z, Hallowita N, Rodgers MT (2005) J Phys Chem A 109:11539–11550
- Tanaka N, Tamezane T, Nishikiori H, Fujii T (2003) J Mol Struct THEOCHEM 631:21–28
- Koné M, Illien B, Graton J, Laurence C (2005) J Phys Chem A 109:11907–11913
- Koné M, Illien B, Laurence C, Graton J (2011) J Phys Chem A 115:13975–13985
- Laurence C, Gal JF (eds) (2009) Lewis basicity and affinity scales: Data and measurement. Wiley, Chichester
- Frisch MJ, Trucks GA, Schlegel HB, Scuseria GE, Robb MA, Cheeseman JR, Montgomery Jr JA, Vreeven T, Kudin KN, Burant JC, Millam JM, Iyengar SS, Tomasi J, Barone V, Mennucci B, Cossi M, Scalmani G, Rega N, Petersson GA, Nakatsuji H, Hada M, Ehara M, Toyota K, Fukuda R, Hasegawa J, Ishida M, Nakajima T, Honda Y, Kitao O, Nakai H, Klene M, Li X, Knox JE, Hratchian HP, Cross JB, Adamo C, Jaramillo J, Gomperts R, Stratmann RE, Yazyev O, Austin AJ, Cammi R, Pomelli C, Ochtersky JW, Ayala PY, Morokuma K, Voth GA, Salvador P, Dannenberg JJ, Zakrzewski VG, Dapprich S, Daniels AD, Strain MC, Farkas O, Malick DK, Rabuck AD, Raghavachari K, Foresman JB, Ortiz JV, Cui Q, Baboul AG, Clifford S, Cioslowski J, Stefanov BB, Liu G, Liashenko A, Piskorz P, Komaromi L, Martin RL, Fox DJ, Keith T, Al-Laham MA, Peng CY, Nanayakkara A, Challacombe M, Gill PMW, Johnson B, Chen W, Wong MW, Gonzalez C, Pople JA (2003) Gaussian 03, Revision B.03. Gaussian, Pittsburgh, PA
- Hill TL (1960) Introduction to statistic thermodynamics. Addison-Wesley, New York
- Halls MD, Velkovski J, Schlegel HB (2001) Theor Chem Acc 105:413–421
- Reed AE, Curtis LA, Weinhold F (1988) Chem Rev 88:899–926
- Bader RFW (1999) Atoms in molecules, a quantum theory. Oxford University Press, Oxford
- Biegler-König FW, Bader RFW, Tang TH (1982) J Comput Chem 3:317–328
- van Duijneveldt FB, van Duijneveldt-van de Rijdt JCM, van Lenthe JH (1994) Chem Rev 94:1873–1885
- Boys SF, Bernardi F (1970) Mol Phys 19:553–566
- Bondi A (1964) J Phys Chem 68:441–451
- Aakeröy CB, Evans TA, Seddon KR, Pálinkó I (1999) New J Chem 23:145–152
- Jiang JC, Tsai MH (1997) J Phys Chem A 101:1982–1988
- Rozas I, Alkorta I, Elguero J (1997) J Phys Chem A 101:9457–9463
- Shi FQ, An JY, Li W, Zhao S, Yu JY (2004) Acta Chim Sinica 62:1171–1175
- Xu LN, Xiao HM, Fang GY, Ju XH (2005) Acta Chim Sinica 63:1062–1068
- Chao J (1986) Int J Thermophys 7:431–442